Catalysis Today 304 (2018) 58–63

Contents lists available at ScienceDirect

Catalysis Today

journal homepage: www.elsevier.com/locate/cattod

Catalysts for conversion of ethanol to butanol: Effect of acid-base and redox properties

Stefano Cimino, Luciana Lisi*, Stella Romanucci

Istituto di Ricerche sulla Combustione, CNR, P.le Tecchio 80, 80125, Naples, Italy

ARTICLE INFO

Keywords:
Ethanol
Butanol
Acid and basic properties
Redox properties
Metal

ABSTRACT

The effect of acid-base properties of three different supports (hydroxyapatite, γ-Al_2O_3 and MgO) and of the redox properties of dispersed Ru or Ni on the catalytic conversion of ethanol into butanol has been investigated.

Catalytic tests have been carried out in the temperature range 200–500 °C by feeding an ethanol/N_2 mixture to a lab-scale fixed bed reactor of powdered catalyst. Both supports and metal containing materials were deeply characterized by XRD, N_2 physisorption, CO_2 and NH_3 TPD, H_2 TPR.

Highest butanol yields were associated to low ratio between acid and basic centres, typical of MgO, and to the easy reducibility of well dispersed metals as well. Good butanol yields can be also ascribed to the enhancement of both surface area and basicity of MgO provided by metal addition.

1. Introduction

In the past decade production of bioethanol from first generation bio-based feedstocks, like corn and sugarcane, significantly increased [1,2]. The use of fuels from these renewable resources offers a lot of environmental benefits, first of all lower greenhouse gas emissions.

Bio-ethanol is used as a fuel additive but, unless modified engines are used, it cannot be used in higher proportion [3] due to its water solubility, corrosivity and low energy content per unit volume compared to gasoline. On the other hand, *n*-butanol can be burned in the existing gasoline engines without basically any engine modification, it has higher calorific value and it can be transported via the existing gasoline pipelines [2]. Consequently, fermentation-derived butanol has attracted renewed interest as a fuel [4]. Biomass fermentation producing *n*-butanol using *Clostridium* microorganisms (Acetone Butanol Ethanol or ABE fermentation) has been performed on the industrial scale in many industrialized countries [4]. Alternatives routes to ABE for butanol production are currently under development although still far from industrial scale. One of them is the catalytic upgrade of ethanol into butanol [5]. The process to increase the carbon number of alcohols is known as Guerbet reaction. In this reaction a primary or secondary alcohol reacts with itself or another alcohol to produce a higher alcohol [5–10].

A suitable combination of both acid and basic sites is considered a key-feature for an effective catalyst for Guerbet reaction. Furthermore, addition of an active metal capable to provide hydrogenation/dehydrogenation properties might promote the initial dehydrogenation of the alcohol to form the carbonyl intermediate of the Guerbet coupling [5].

Solid bases [11], zeolites [12] and supported metals (e.g., Ni, Co) [13,14] have been reported to convert ethanol to *n*-butanol. One of the most investigated catalyst is hydroxyapatite (HAP) with different Ca/P molar ratios [9,15] or with Ca substitution [16].

On the other hand, different metals (Ru, Rh, Pd, Pt, Au, Ni, Ag) over alumina were reported to produce 1-butanol from ethanol via a one-pot liquid-phase reaction [14].

Basic mixed oxides are mostly based on MgO [6,10,17,18]. Modification of MgO, as mixed oxides Cu−Mg−Al, was also attempted [18]. It was found that the selectivity to 1-butanol increased with the number of strong basic sites. Similar conclusions were drawn about Mg−Al mixed oxides derived from hydrotalcites [18]. Catalysts with higher concentration and strength of the basic sites lead to high selectively to C4 products whereas the presence of acid sites promotes ethanol dehydration. One of the methods to increase these acid−base pairs is by incorporation of stronger Lewis acid like Al into Mg [5].

Nevertheless, acidic properties were also found to be essential for the production of 1-butanol. It was demonstrated that adjacent acid and medium basic sites can generate intermediate compounds leading to 1-butanol formation [19].

It is generally accepted that the Guerbet reaction is a sequence of different reactions starting from dehydrogenation of alcohol, followed by aldol condensation, dehydration and finally hydrogenation of the unsaturated aldehyde. [5].

In their recent review Chieregato et al. [19] described the reaction

* Corresponding author.
E-mail address: lisi@irc.cnr.it (L. Lisi).

http://dx.doi.org/10.1016/j.cattod.2017.08.035
Received 5 June 2017; Received in revised form 17 July 2017; Accepted 14 August 2017
Available online 25 August 2017

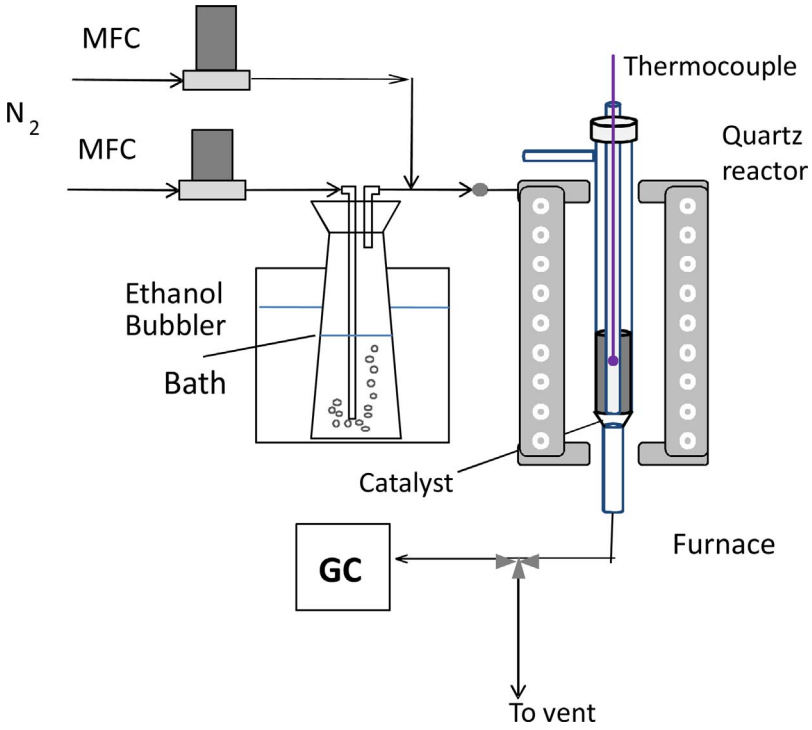

Fig. 1. Sketch of the experimental rig for catalysts screening.

mechanism occurring on MgO analyzing the catalyst features necessary to address the process towards Guerbet instead of Lebedev reaction, which means towards butanol instead of butadiene. During Guerbet coupling over basic catalysts as MgO one of the major hurdles is the initial dehydrogenation of the alcohol to form the carbonyl intermediate, which explains why addition of a hydrogenation/dehydrogenation catalyst such as copper improves the performance of basic metal oxide catalysts.

At least two reaction pathways are suggested to take place simultaneously on hydroxyapatite in the temperature range 350–410 °C by Scalbert et al. [20], a main pathway (direct route) involving the condensation of two ethanol molecules with apparently no intermediate gaseous compounds, and an indirect route involving the condensation of ethanol with acetaldehyde (formed from ethanol dehydrogenation) to form butenol, which is subsequently converted to butanol by hydrogen transfer from a sacrificial ethanol molecule.

All these results globally suggest that catalysts composed of a basic support and a transition metal can have an advantage over basic metal oxides for the Guerbet reaction. Use of a metal promoter enhances the ability, in some instances, to operate at lower temperatures because the dehydrogenation of the alcohol occurs much more readily over metals than over metal oxides such as MgO [2].

In this work we set out to investigate the effect of acid-base properties of several supports such as hydroxyapatite, MgO and γ-Al_2O_3 on butanol production from ethanol. The effect of dispersion of small (≤1%) amounts of ruthenium or nickel was also studied and acid-base properties of the supports and redox properties of the metal were correlated to the catalytic performance.

2. Materials and methods

Hydroxyapatite (HAP) was synthesized mixing two aqueous solutions containing calcium nitrate tetrahydrate ($Ca(NO_3)_2{\cdot}4H_2O$ and diammonium phosphate ($(NH_4)_2HPO_4$) with stoichiometric molar ratio of Ca/P (1.67) adjusting pH to 10. Suspension was stirred for 24 h at 70 °C and then the precipitate dried after separation at 120 °C and calcined at 600 °C under air for 2 h [9].

γ-Al_2O_3 powder was a commercial (SCF-140) powder supplied by SASOL.

MgO powder was obtained starting from $Mg(NO_3)_2$ solution precipitating magnesium hydroxide by addition ammonia solution (25%) with 5:1 NH_3/Mg ratio. The precipitate was stirred at 60 °C for 6 h in a closed bottle according to [21]. Centrifugated powder was dried at 120 °C overnight and calcined at 450 °C for 2 h.

Ruthenium was dispersed on HAP, γ-Al_2O_3 and MgO powder by wet impregnation starting from ruthenium from nitrosyl nitrate. Nickel was dispersed on MgO from nitrate solution.

Supports were characterized by XRD analysis performed on powder samples with a Bruker D2 Phaser diffractometer (operated at diffraction angles ranging between 10 and 80° 2θ with a scan velocity equal to 0.02° 2θ s^{-1}).

BET specific surface area measurements were performed with a Quantachrome Autosorb 1-C by N_2 adsorption at 77 K after degassing samples for 2 h at 150 °C.

Temperature programmed reduction (TPR) experiments were carried out with a Micromeritics AutoChem 2020 equipped with a TC detector on catalysts and supports pre-treated in air at 600 °C. The sample powder (150 mg) was heated at 10 °C min^{-1} between room temperature and 900 °C in flowing 2% H_2/Ar mix (50 cm^3 min^{-1}). CO_2 and NH_3 TPD were carried out using the same apparatus pre-treating the sample under the same condition and, after adsorption at room temperature of the probe molecule (CO_2 or NH_3), the sample was heated at 10 °C min^{-1} up to 600 °C under He flow (50 cm^3 min^{-1})

Catalytic tests were carried out in the temperature range 200–500 °C by feeding an 3% vol. ethanol/N_2 mixture to a lab-scale fixed bed reactor of 0.8 g powdered catalyst (300–400 μm). Very diluted conditions, although not favourable for high butanol yield, were chosen in order to avoid condensation of products in the cold pipelines which can easily take place especially for heavier products such as butanol or crotonaldehyde.

Reactants and products were analysed by an online GC (Hewlett Packard 1540A) equipped with FI detector and a ZB-WAX*plus* column. All species were separated except for ethylene from diethylether. As a consequence, the species corresponding to this peak will be reported below as diethylether/ethylene.

Ethanol conversion was reported as ethanol reacted/ethanol

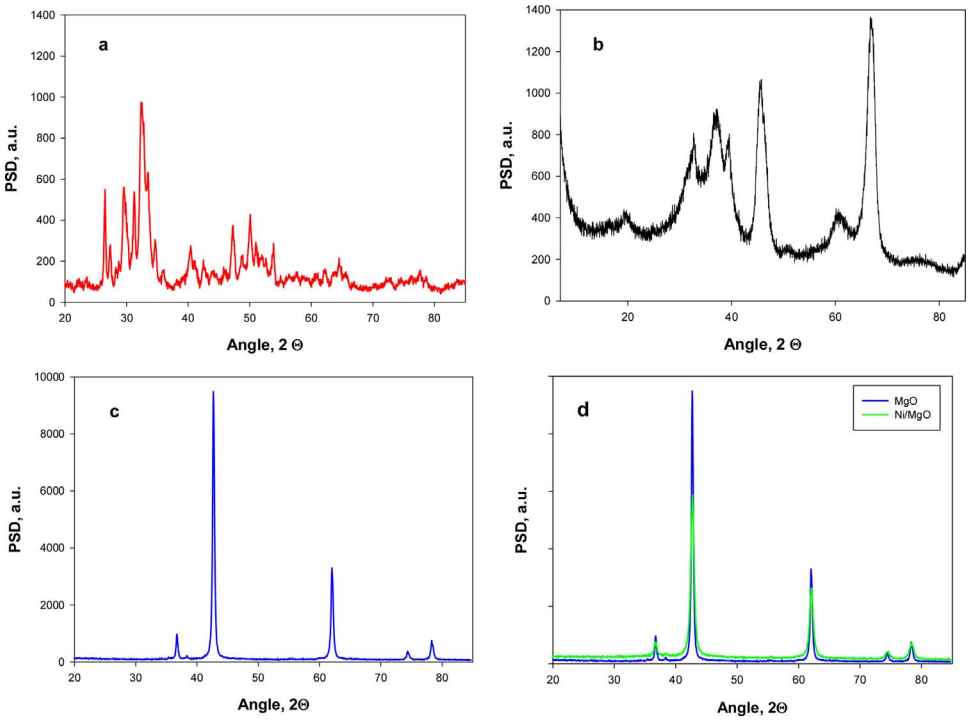

Fig. 2. XRD patterns of a) calcined HAP (red), b) γ-Al_2O_3 (black) and c) MgO (blue). D) Comparison between MgO and Ni/MgO (green). (For interpretation of the references to colour in this figure legend, the reader is referred to the web version of this article.)

introduced x 100 (vol./vol.). Butanol selectivity was expressed as butanol produced/ethanol reacted x 100 (vol./vol.).

A sketch of the test rig is reported in Fig. 1. The reactor was operated at nearly atmospheric pressure, under pseudo-isothermal conditions. An ethanol/N_2 mixture was prepared by mixing two N_2 streams, independently regulated by mass flow controllers, one passing through an ethanol saturator at room temperature.

3. Results and discussion

In Fig. 2 a, c XRD patterns of HAP and MgO after calcination are reported showing the typical reflections of the hydroxyapatite and MgO phases, MgO showing a much higher crystallinity. Commercial alumina shows quite broad γ-Al_2O_3 signals indicating a low crystallinity (Fig. 2b) Small signals corresponding to.

In Table 1 BET surface areas of supports and catalysts are reported. In contrast with commercial alumina, having a quite high surface area, both HAP and MgO show a small area. Nevertheless, whilst addition of a small fraction of metal results in a reduction of original surface area of alumina, the same addition does not significantly affect the BET area of HAP and causes a large increase of the original surface area of MgO (adding both Ru and Ni). As expected, the increase of surface area of MgO is coupled to a partial loss of crystallinity of this support as shown by the comparison of XRD pattern of pure MgO and Ni/MgO (Fig. 2d).

Table 1
BET surface area of both supports and catalysts and amount of CO_2 and NH_3 desorbed from supports in TPD experiments.

Sample	BET area	CO_2 (TPD)		NH_3 (TPD)	
	$m^2\,g^{-1}$	mmol g^{-1}	μmol m^{-2}	mmol g^{-1}	μmol m^{-2}
HAP	37	0.037	1.0	0.23	6.2
γ-Al_2O_3	140	0.076	0.54	0.73	5.2
MgO	26	0.064	2.9	0.13	5.9
1%Ru/HAP	24	–	–	–	–
1%Ru/Al_2O_3	132	–	–	–	–
0.16% Ru/MgO	63	–	–	–	–
1%Ni/MgO	75	–	–	–	–
0.47%Ni/MgO	92	–	–	–	–

CO_2 TPD of supports (Fig. 3) indicated the presence of weak basic sites associated to a peak centred at about 120 °C. MgO shows an additional peak with respect to alumina and HAP at slightly higher temperature.

On the other hand, alumina shows a more complex NH_3 TPD profiles with at least two contributions at low and high temperature. The very weak acid sites give rise to a signal peaked at 110 °C whilst strong acid sites are associated to a broad signal centred at about 400 °C and extending up to 600 °C. On the contrary, HAP shows a single tailed peak centred at about 150 °C.

In Table 1 the results of the integration of TPD profiles are reported as moles of CO_2 or NH_3 both per unit weight and per unit surface. Alumina adsorbs a large amount of ammonia that, if related to the surface area, is not so high whereas it has a low contribution of basic sites, also considering the BET area. Thus, for alumina a strong dominance of acid sites with respect to basic sites was observed. On the other hand, MgO is the support with the higher ratio between surface concentration of basic sites with respect to acid sites.

In Fig. 4H_2 TPR profiles of ruthenium dispersed on the three supports are reported. Comparison of profiles clearly shows a great difference of the temperature range for metal reduction. Ruthenium dispersed on alumina is very easily and completely reduced at very low temperature. Higher temperature is required for ruthenium on HAP and MgO respectively, likely related to a worse metal dispersion on supports with a lower surface area compared to alumina. Nevertheless, this reason could not be the only one for Ru on MgO due to the increase of the surface area detected upon metal deposition by wet impregnation.

Preliminary catalytic tests have been performed on bare supports. The main products detected were, in addition to butanol, acetaldehyde, crotonaldehyde, diethylether/ethylene. Conversion of ethanol as a function of temperature is reported in Fig. 5.

HAP showed a negligible activity up to 300 °C whereas between 300 and 400 °C an almost complete conversion of ethanol was observed. Indeed, no butanol was detected among products mainly consisting in diethylether/ethylene with traces of acetaldehyde and crotonaldehyde. Likewise, γ-Al_2O_3, although providing a high ethanol conversion already at 300 °C, mostly produces diethylether/ethylene associated to

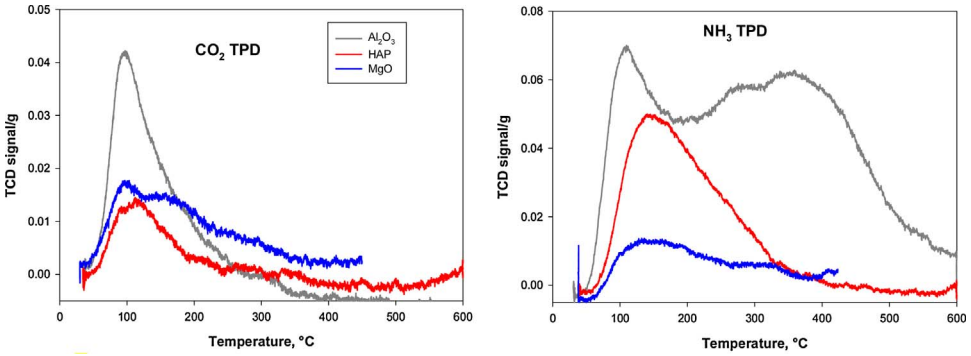

Fig. 3. CO_2 and NH_3 TPD profiles of calcined HAP, γ-Al_2O_3 and MgO.

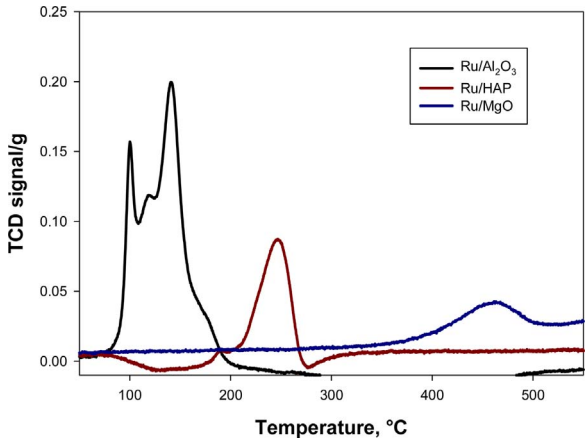

Fig. 4. H_2 TPR profiles of Ru/HAP, Ru/Al_2O_3 and Ru/MgO.

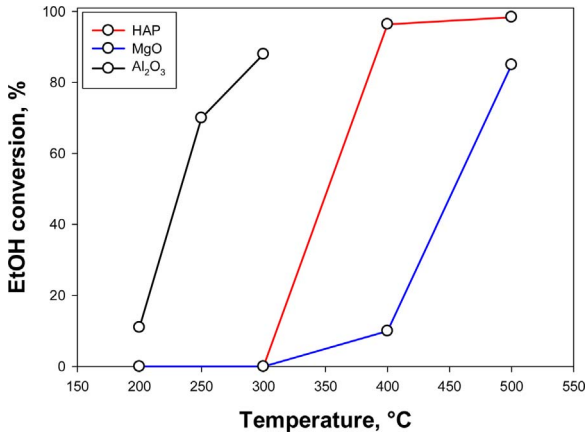

Fig. 5. Ethanol conversion as a function of temperature for HAP, Al_2O_3 and MgO.

traces of aldehydes, all products increasing with reaction temperature.

Ethanol conversion on MgO is definitely lower and occurs at higher temperature, however, this material shows an intrinsic activity towards butanol production. The different reaction path promoted by MgO with respect to the other two supports is also demonstrated by the detection of a transient period when negligible ethanol exit concentration was detected not corresponding to a simultaneous production of any products. This clearly suggests that saturation of MgO surface is taking place. Only when saturation was completed butanol started to be produced.

Butanol production increases with temperature (0.015% vol. at 500 °C) and the same occurs for the other products, however, production of acetaldehyde is higher than that observed for the other two supports. Butanol selectivity shows a maximum at 400 °C (4.0%).

Chieregato et al. [19] reported that the formation of 1-butanol is promoted by catalysts able to stabilize the first intermediate, i.e. the carbanion formed upon ethanol adsorption on MgO. and by the lack of acetaldehyde on the vicinal sites. A vicinal adsorbed acetaldehyde can give butadiene instead of 1-butanol (i. e. Lebedev reaction instead of Guerbet reaction) whereas an excessive stabilization of the carbanion can lead to ethylene formation.

In the experiments carried out in this work butadiene was never detected whereas formation of ethylene apparently competes with butanol formation.

The addition of ruthenium does not improve performance of HAP whereas results in the appearance of butanol among the reaction products for γ-Al_2O_3 that, although with low selectivity (1.6-1.7% at 200–250 °C), suggests a key-role of the metal. On the other hand, dispersion of a small fraction of metals increases ethanol conversion for MgO and this improvement was also observed substituting Ru for Ni (Fig. 6). That is seemingly in contrast with Ndou et al. [11] who investigated the effect of the addition of transition metals as Zn, Ce, Zr, Pb, Sn to MgO which did not provide better performance.

Furthermore, a significant increase (about 5 times greater volume concentration at 400 °C) of butanol production was obtained by adding a low Ni amount which results in a double butanol selectivity at 400 °C (8.0%) (Fig. 7).

Although the increase of surface area upon metal dispersion could suggest that the enhanced performance can be related to a larger surface available for ethanol coupling, that could not be the only reason associated to the better performance. Actually, different properties changed upon metal addition. First of all, metals can play a specific role in the reaction path [5,19], as also confirmed by the results obtained on alumina supported ruthenium. To this end, reducibility of Ru/MgO and Ni/MgO was evaluated by H_2 TPR analysis. Comparison of corresponding TPR profiles is reported in Fig. 8.

Both ruthenium and nickel undergo reduction starting at

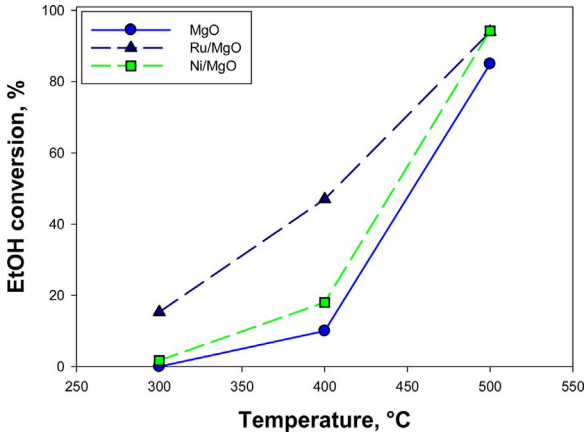

Fig. 6. Ethanol conversion as a function of temperature for MgO, 0.16% Ru/MgO and 0.47% Ni/MgO.

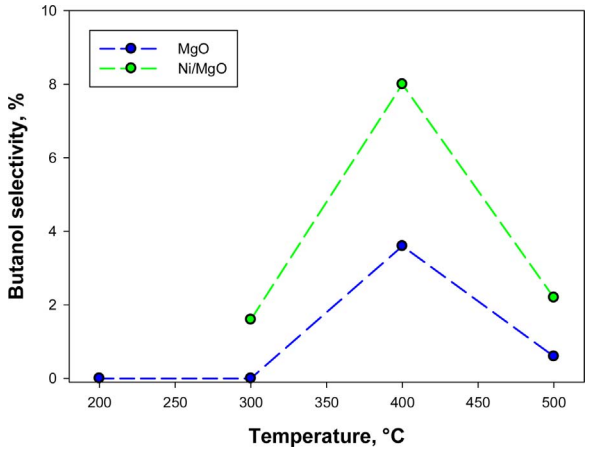

Fig. 7. Butanol selectivity as a function of reaction temperature for MgO and Ni/MgO.

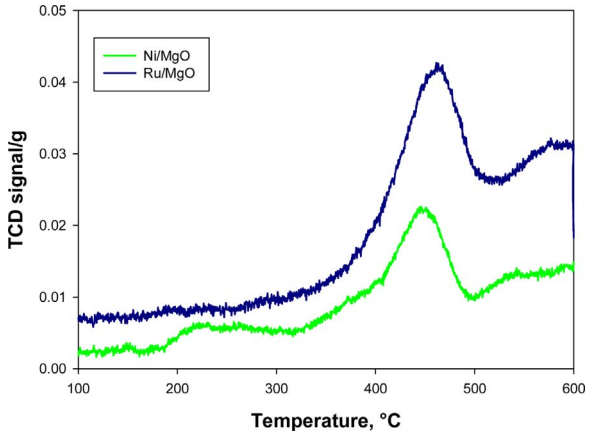

Fig. 8. H_2 TPR profiles of Ru/MgO and Ni/MgO.

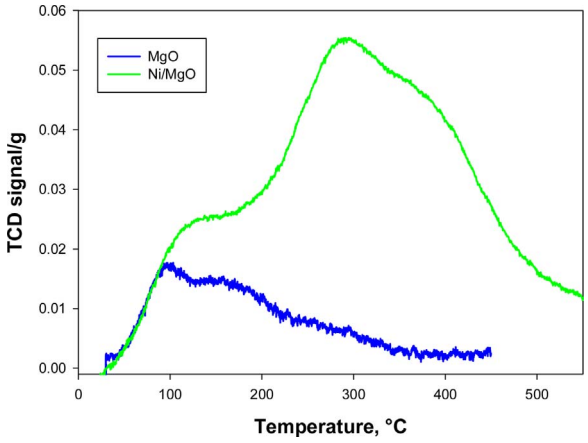

Fig. 9. Comparison of CO_2 TPD profiles of calcined MgO and Ni/MgO.

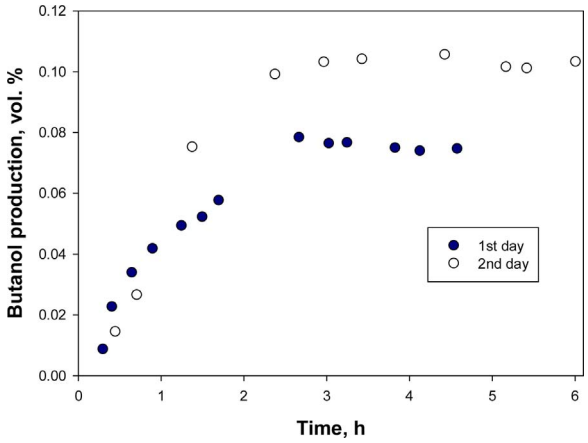

Fig. 10. Butanol production at 400 °C over Ru/MgO with time on stream. Comparison between results of the 1st day and those of the 2nd day under the same operation condition.

T > 300 °C giving a peak at about 450 °C. The best butanol selectivity obtained in the same range of metal reduction could suggests that metals are involved in butanol production. Nevertheless, the maximum butanol selectivity was observed in the same temperature range also for pure MgO, as shown in Fig. 7, thus suggesting also an indirect effect of metal addition.

Ueda et al. [22] reported that addition of various transition metals, different from that explored by Ndou et al. [11], to MgO provided extra basicity which was maximum for Ni and Cu. As a consequence, a more indirect role of the dispersed metal cannot be ruled out. On the other hand, Ndou et al. [11] proposed that C—H bond in the β-position in ethanol, activated by the basic metal oxide, condenses with another molecule of ethanol by dehydration to form 1-butanol, thus underlining the key role of basic sites.

The enhanced basicity was confirmed by the comparison of CO_2 TPD test of MgO and Ni/MgO (Fig. 9). The addition of the metal strongly increases the number and the nature of basic sites providing additional sites desorbing CO_2 especially in the range 250–600 °C. The amount of the basic centers increases from 0.064 mmol g^{-1} to 0.28 mmol g^{-1}. This is only partially assignable to the enhanced surface area of the metal containing MgO. Indeed, if this amount refers to the surface area an increase from 2.9 to 3.8 μmol m^{-2} is evaluated thus suggesting that some basicity is also related to a modification of properties of MgO provided by metal addition. As a consequence, a single effect of metal addition on increased butanol production cannot be found and additional experiments are necessary to possibly exclude or confirm one or more effects (Fig. 9).

Finally, in order to test catalysts stability a 5 h test was carried out at 400 °C over Ru/MgO catalyst which was interrupted and resumed the next day under the same operating condition and carried on for further 6 h. A surprising increase of steady state performance was observed with time on stream, as shown in Fig. 10.

Actually, stable performance was reached after about 2–3 h during the test carried out in the first day. The day before a transient period was detected again, however, a higher steady-state value of butanol production was observed suggesting some catalyst activation likely related to the contact with water produced through the coupling reaction which could further increases the surface area and/or further promotes the positive interaction between MgO and the metal.

4. Conclusions

Supports with different acid and basic properties have been investigated for the catalytic conversion of ethanol into butanol in the temperature range 200–500 °C. Alumina and hydroxyapatite can convert ethanol at quite low temperature under the operative condition explored but mostly providing diethylether/ethylene. MgO is the only material showing an intrinsic activity towards butanol production due to dominance of basic centres on acid ones. Performance is further enhanced by metal (Ru or Ni) addition thanks to a simultaneous increase of surface area and basicity. On the other hand, reduction of the metal in the same operation temperature range of the reaction can also suggest a contribution of redox properties of the metal promoting the hydrogenation/dehydrogenation step of the reaction path. A surprising activation of metal-promoted MgO was observed by repeating the catalytic test on the material tested the day before likely associated to a

favourable effect of water produced by the coupling reaction.

Acknowledgements

The work has been done in the framework of the research project Waste2Fuels 'Sustainable production of next generation biofuels from waste streams' (N. 654623) funded under the European Union's research and innovation program Horizon 2020. Authors are grateful to Mr. Ferdinando Stanzione (IRC—CNR) for his support in gas-chromatografic analyses and to Mr.Luciano Cortese for XRD analysis.

References

[1] A.D. Patel, S. Telalović, J.H. Bitterb, E. Worrell, M.K. Patel, Catal. Today 239 (2015) 56–79.
[2] J. Sun, Y. Wang, A.C.S Catal 4 (2014) 1078–1090.
[3] J.H. Earley, R.A. Bourne, M.J. Watson, M. Poliakoff, Green Chem. 17 (2015) 3018–3025.
[4] P.H. Pfromm, V. Amanor-Boadu, R. Nelson, P. Vadlani, R. Madl, Biomass Bioenergy 34 (2010) 515–524.
[5] J.T. Kozlowski, R.J. Davis, A.C.S Catal. 3 (2013) 1588–1600.
[6] J.L.M. Gines, E. Iglesia, J. Catal. 176 (1998) 155–172.
[7] W. Ueda, T. Ohshida, T. Kuwabara, Y. Morikawa, Catal. Lett. 12 (1992) 97–104.
[8] C. Carlini, M. Marchionna, M. Noviello, A.M. Raspolli Galletti, G. Sbrana, F. Basile, A. Vaccari, J. Mol. Catal. A 232 (2005) 13–20.
[9] T. Tsuchida, S. Sakuma, T. Takeguchi, W. Ueda, Ind. Eng. Chem. Res. 45 (2006) 8634–8642.
[10] W. Ueda, T. Kuwabara, T. Ohshida, Y.A. Morikawa, J. Chem. Soc Chem. Commun. (1990) 1558–1559.
[11] A.S. Ndou, N. Plint, N.J. Coville, Appl. Catal. A Gen. 251 (2003) 337–345.
[12] C. Yang, Z. Meng, J. Catal. 142 (1993) 37–44.
[13] K.W. Yang, X.Z. Jiang, W.C. Zhang, Chin. Chem. Lett. 15 (2004) 1497–1500.
[14] T. Riittonen, E. Toukoniitty, D. Kumar Madnani, A.R. Leino, K. Kordas, M. Szabo, A. Sapi, A.K. Arve, J. Wärnå, J.P. Mikkola, Catalysts 2 (2012) 68–84.
[15] T. Tsuchida, J. Kuboa, T. Yoshioka, S. Sakuma, T. Takeguchi, W. Ueda, J. Catal. 259 (2008) 183–189.
[16] S. Ogo, A. Onda, K. Yanagisawa, Appl Catal. A Gen. 402 (2011) 188–195.
[17] I.-C. Marcu, D. Tichit, F. Fajula, N. Tanchoux, Catal. Today 147 (2009) 21–238.
[18] D.L. Carvalho, R.R. de Avillez, M.-T. Rodrigues, L.E. Borges, L.G. Appel, Appl. Catal. A 415 (2012) 96–100.
[19] A. Chieregato, J. Velasquez Ochoa, C. Bandinelli, G. Fornasari, F. Cavani, M. Mella, ChemSusChem 8 (2015) 377–388.
[20] J. Scalbert, F. Thibault-Starzyk, R. Jacquot, D. Morvan, F. Meunier, J. Catal. 311 (2014) 28–32.
[21] A. Hanif, S. Dasgupta, A. Nanoti, Ind. Eng. Chem. Res. 55 (2016) 8070–8078.
[22] W. Ueda, T. Yokoyama, Y. Moro-Oka, T. Ikawa, Chem. Lett. (1985) 1059–1062.